THE JOURNAL OF PROSTHETIC DENTISTRY

RESEARCH AND EDUCATION

Biomechanical analysis of 4 types of short dental implants in a resorbed mandible

Hyeonjong Lee, DMD, MSD, PhD,[a] Soyeon Park, BS,[b] and Gunwoo Noh, PhD[c]

ABSTRACT

Statement of problem. Short implants have been increasingly used in the aging society. However, studies which explain the difference of stress distribution according to different connections in short implant treatment are scarce.

Purpose. The purpose of this finite element (FE) analysis was to evaluate the stress and strain distribution of short implants and surrounding bone under static and cyclic loading conditions with 4 different connections.

Material and methods. Three-dimensional models of 4 types of implant systems were considered: internal tissue level, internal tissue level wide, internal bone level (IB), and external bone level. Each system had different types of abutment, implant, and screw with the resorbed mandibular segment of the bone block. Static FE analysis was performed under external loads of 200 N (vertical or 30-degree oblique) to each cusp tip. The strain distributions of the peri-implant bone and von Mises stress fields in the abutment, implant, and screw were evaluated. Based on the static FE results, a computational fatigue analysis was performed to predict the risk of fracture caused by fatigue accumulation of repetitive mastication.

Results. Bone tissues in fatigue failure level (greater than 4000 με) were observed in the alveolar ridge and the plateaus close to the implant apex in all situations. Under the oblique loading condition, the total volume of the bone tissue in hypertrophy and fatigue failure levels (greater than 2500 με) was the largest at IB and the smallest at external bone level. Among the 4 situations, the highest stress occurred in the abutment (506.9 MPa) and implant (311 MPa) of IB. In fatigue analysis, fracture was only predicted in the IB abutment model (588 301 cycles), and cracking occurred in the lingual direction, where stress concentration occurred when the oblique load was applied.

Conclusions. The abutment of IB showed the highest stress of the implant component, and internal tissue level model showed the highest strain of bone. In all groups, the bone strain values mostly appeared within physiologic capacity (under 4000 με). Various mechanical situations should be considered when using internal bone-level connections in short implants for replacing posterior teeth. (J Prosthet Dent 2019;121:659-70)

Recently, short implants have been used to reduce the need for bone grafting. The implant and prosthetic survival rate of short implants is similar to that of longer implants in vertically augmented bone[1,2]; however, randomized clinical controlled studies that compare the procedures are lacking.

Finite element analysis (FEA) studies have evaluated the stress distribution of the implant, abutment, and surrounding bone under various conditions.[3-16] The effects of different abutment connection designs on the stress distribution around the implants have been reported.[3-11,16] When short implants are installed in a reduced alveolar ridge with various connection types such as internal, external bone, or tissue-level connection, the stress distribution of the implant component and surrounding bone would differ according to different connections. However, studies of biomechanical analysis depending on different connections in short implants are scarce.

The crown/implant (C/I) ratio is an important factor in implant restoration.[17] A high C/I ratio is related to the high-lever effect on the implant restoration under non-axial loading, which might lead to technical problems.[18-20]

This study was supported by the Basic Science Research Program through the National Research Foundation of Korea (NRF) funded by the Ministry of Education (grant no.: NRF-2018R1D1A1B07049789).

[a]International Scholar, Department of Fixed Prosthodontics and Biomaterials, School of Dental Medicine, University of Geneva, Geneva, Switzerland.
[b]Graduate student, School of Mechanical Engineering, Kyungpook National University, Daegu, Republic of Korea.
[c]Assistant Professor, School of Mechanical Engineering, Kyungpook National University, Daegu, Republic of Korea.

Clinical Implication

A more than 2-fold difference was obtained in the stress on implant components depending on the connection and nearly a 3.5-fold difference according to the different loading directions. In selecting short implants, the off-axis load and connections should be considered.

From the biological aspect, the correlation between the C/I ratio and marginal bone loss is unclear.[21-23] A lower marginal bone loss at higher C/I ratio has been reported in some studies,[21,22] whereas others have reported the opposite.[23,24] The anatomic C/I ratio was used in some studies,[25,26] whereas the clinical C/I ratio was used in others.[21,27] Both ratios have different implications from a mechanical aspect. When bone-level and tissue-level implant restorations have the same clinical C/I ratio, the anatomic C/I ratio of the tissue-level implant could be reduced compared with the bone-level implant because of the length of the transmucosal part, which decreases the length of the anatomic crown.

The stress distribution of the surrounding bone has been explained on the basis of the crown height rather than the C/I ratio.[28,29] In view of the lever effect, the clinical crown height of the implant is more meaningful than the C/I ratio in explaining the stress concentration of cortical bone. The diameter of the connection is another important factor for understanding the lever effect. It changes the length and degree of the lever arm as well as the position of the fulcrum, which has not been elucidated in detail.

To the best of the authors' knowledge, FEA that evaluated the stress distribution of the implant, abutment, and bone, considering connection types and fatigue analysis in short implants, has not been previously conducted. Therefore, the purpose of this FEA study was to analyze the stress and strain distribution of short implants and surrounding bone under static and cyclic loading conditions with 4 different connections. The null hypothesis was that no differences in the stress and strain distributions would be found among the 4 connection types.

MATERIAL AND METHODS

Three-dimensional models were prepared for analysis, and 4 types of implant assembly with the resorbed mandibular segment of the bone block were considered. FEA was performed under external loads of 200 N, and the strain distributions of the peri-implant bone and von Mises stress fields in the abutment, implant, and screw were evaluated.

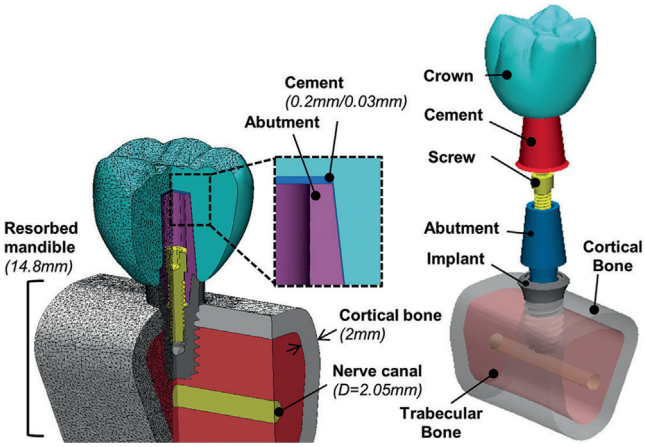

Figure 1. Cross-sectional view of 3D models showing internal structure and cement layer. Inset: Structure of implant components implanted in second molar region.

The bone structure with the inferior dental nerve of a resorbed posterior mandible was modeled by using a 3D modeling software program (Materialise 3-Matic 9.0; Materialise Group). The cortical bone had a thickness of 2 mm, and the inferior dental nerve canal was located 1 mm below the apex of the implant (Fig. 1).[30] The assembly of implant components was implanted in the second molar region and contained a layer of cement (Fig. 1).

The design of the implant models was provided by the manufacturer (TSIII SA, SSIII, USIII; Osstem Implant Co Ltd). Figure 2 showed the dimensions of 4 types of implant system; internal tissue level (IT), internal tissue level wide (ITW), internal bone level (IB), and external bone level (EB). Each system used the same implant length, implant diameter, and total length but used different types of abutment, implant, and screw. The different abutment types were used according to the implant type; IT and ITW had an internal octagon abutment (ComOcta; Osstem Implant Co Ltd), IB had a Morse-tapered internal hexagon abutment (Transfer abutment; Osstem Implant Co Ltd), and EB had an external hexagon abutment (Cement abutment; Osstem Implant Co Ltd). Each crown and cement layer was modeled by proper scaling. All geometries were exported to the FEA software (ABAQUS 6.14; Dassault Systèmes SIMULIA Corp) by using 4 node tetrahedral elements.

The components of the implant system and the surrounding bone were assumed to be isotropic, homogenous, and linearly elastic. Material properties were presented in Table 1.[31-36] The cement layer was thin, at 0.1 mm, whereas the bone fragments and crown components were divided into 0.25- to 1-mm-sized parts to place the smaller elements closer to the implant. Other titanium components were discretized by elements with a minimum size of 0.25 mm. The total number of

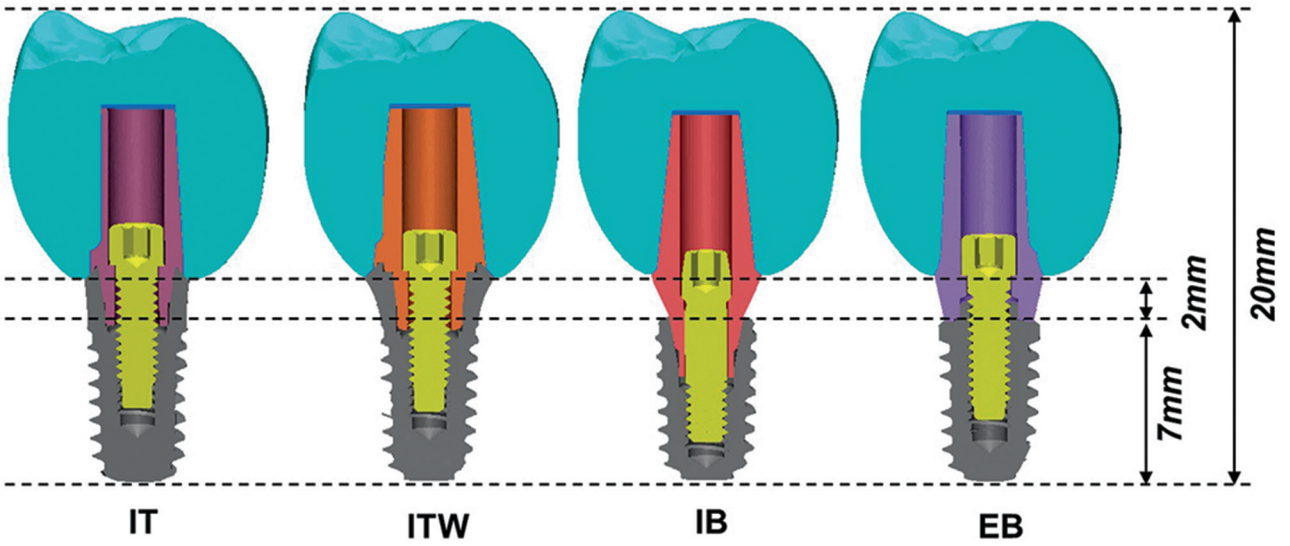

Figure 2. Dimension of 4 types of implant components. Each system used same implant length, diameter, and total length but different types of abutment, implant, and screw. EB, external bone level; IB, internal bone level; IT, internal tissue level; ITW, internal tissue level wide.

Table 1. Material properties used in finite element models

Material Component	Elastic Modulus (MPa)	Poisson Ratio	Reference
Crown	140 000	0.28	Vaillancourt et al[31]
Ti-grade 4	110 000	0.34	Niinomi[33] and Bulaqi et al[32]
Cortical bone	13 700	0.3	Sertgoz[34]
Trabecular bone	1370	0.3	Sevimay et al[35]
Nerve canal	70	0.45	Vaillancourt et al[31]
Cement	10 760	0.35	Tolidis et al[36]

elements used for each model ranged from 1 444 688 to 1 603 982.

For interaction conditions, the abutment and implant were tightly connected to each other by tightening the screw; thus, the area of the tightly engaged surfaces differs for different abutment types. All contact areas between the screw, abutment, and implant were stimulated by contact conditions with a friction coefficient of 0.16.[37] Contact analysis ensured the transfer of load and deformation between all titanium-titanium interfaces. To simulate perfect osseointegration, all interactions incorporating implant and bone were simulated as tied conditions. The tied condition was also used for crown-cement and cement-abutment interfaces.

The boundary conditions were established as fixed in all axes (x, y, and z) at the distal and mesial plane in the block section (Fig. 3). Two loading conditions were considered: (1) a total force of 200 N applied to 60 nodes on 3 cusps in the vertical direction and (2) 200 N to 30 nodes on 3 cusps and 3 fossae in the 30-degree oblique direction (Fig. 3).[38,39]

To predict the risk of fracture caused by the fatigue accumulation of repetitive mastication, a computational fatigue analysis was performed under the 2 loading

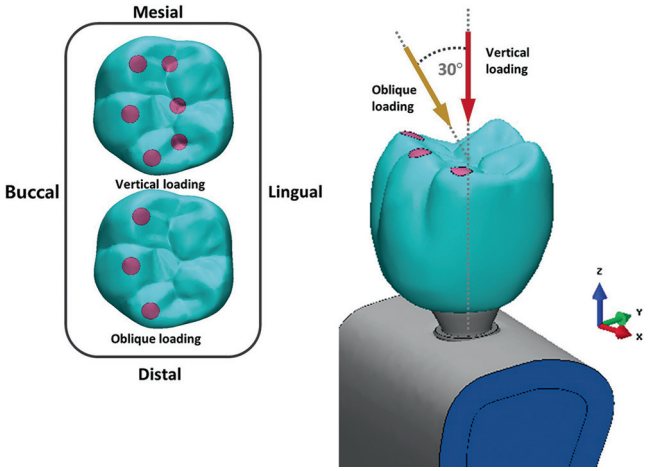

Figure 3. Boundary conditions and load conditions of FE model. Both ends of bone block (blue) fixed in all directions, and total force of 200 N applied to each of 60 nodes on 3 cusps in vertical direction and each of 30 nodes on 3 cusps and 3 fossae in oblique direction. FE, finite element.

conditions. A multiaxial fatigue algorithm incorporating a multiaxial plasticity model with the stress results obtained from the FEA was used in a computer program (FE-Safe v6.5; Safe Technology Ltd). This required the extrapolation of the stresses obtained from FEA at the integration points to the nodes of finite elements.[40] In this study, fatigue calculations of the implant components were conducted for the parts made of grade 4 titanium (Table 1).[33]

The principal strain was used to evaluate the stability of the cortical and trabecular bones. Volume fractions according to strain levels of bone remodeling were estimated using the Frost mechanostat theory, where bone remodeling activity is controlled by the peak strain of

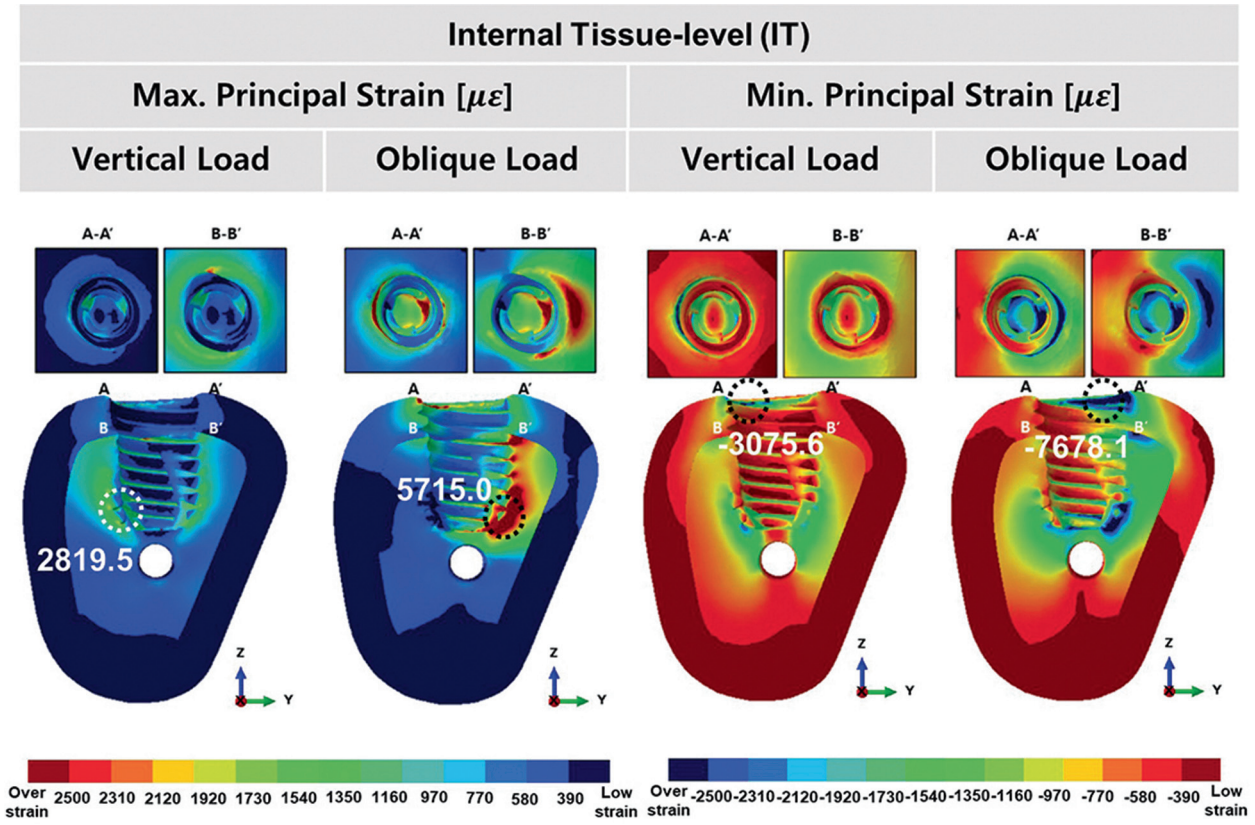

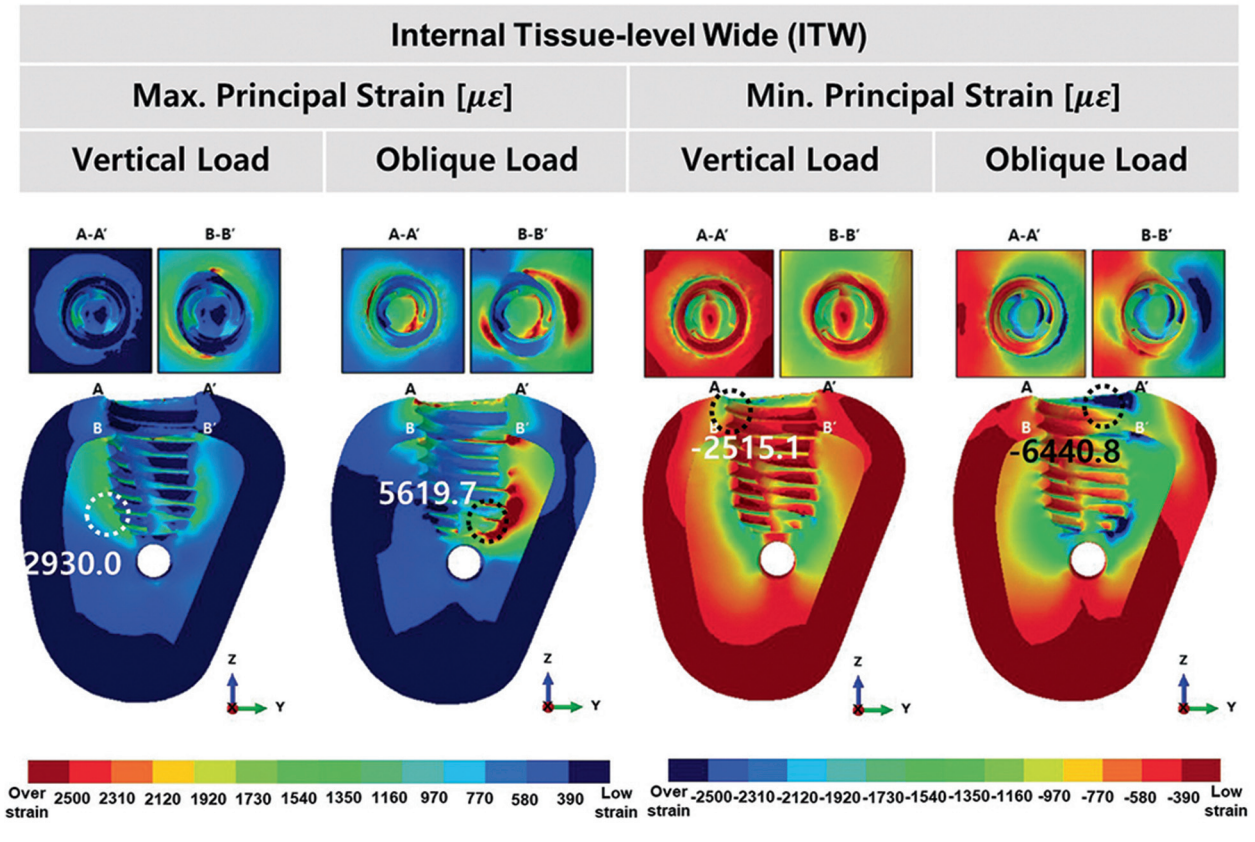

Figure 4. Maximum and minimum principal strain distribution of cortical bone and trabecular bone according to strain levels induced by short implants under 2 loading conditions. A, Internal tissue level. B, Internal tissue level wide. *(Continued on page 663.)*

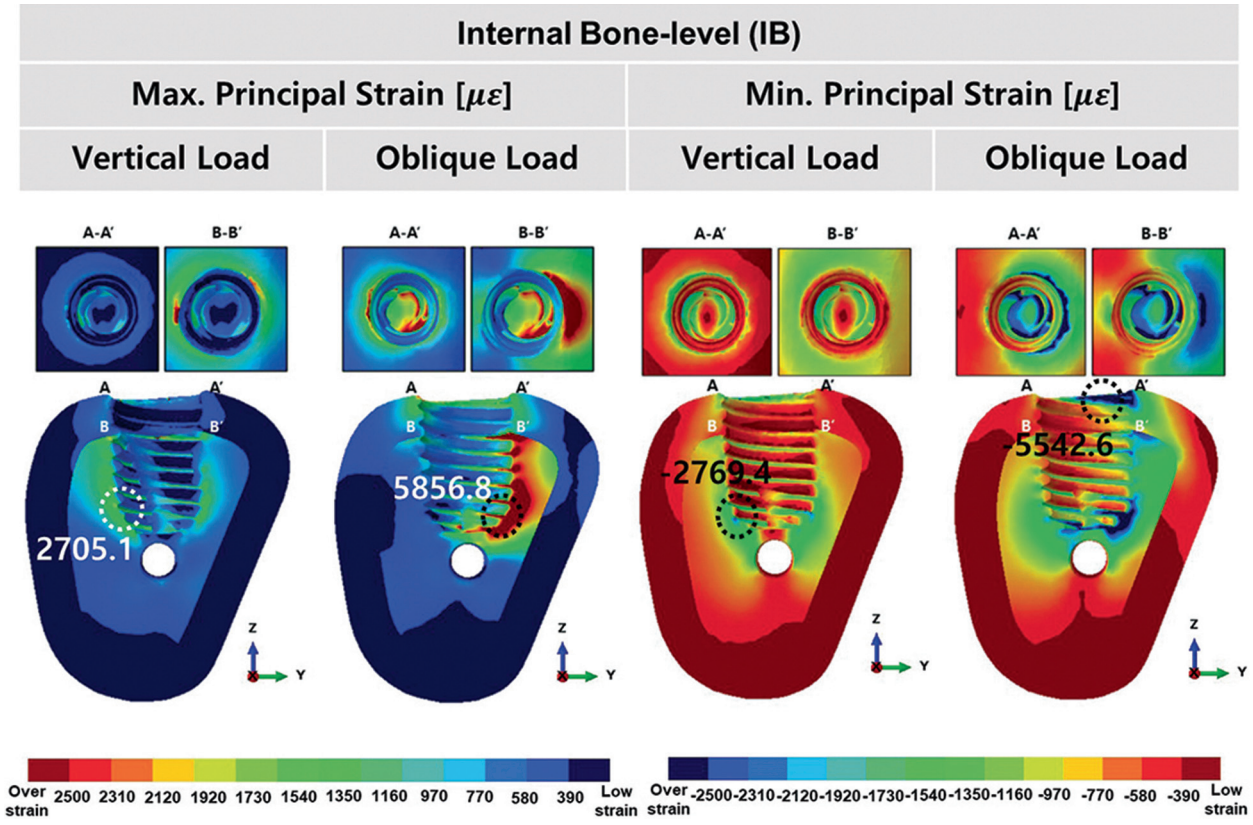

C

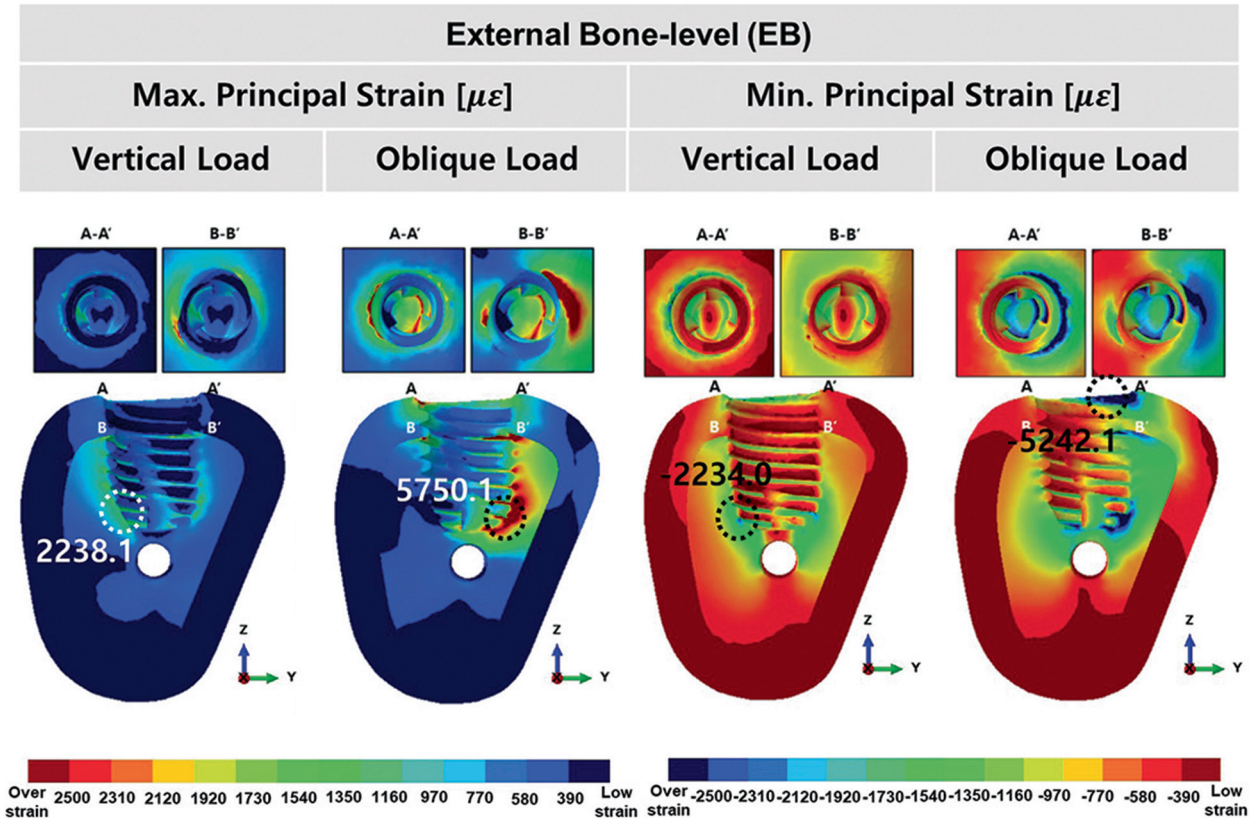

D

Figure 4. (*continued*). C, Internal bone-level. D, External bone-level. Section A-A′ represents upper surface of cortical bone, and B-B′ represents interface between cortical bone and trabecular bone.

dynamic loading. The bone remains in the maintenance level when the strain is in the range of 200 to 2500 με, whereas prolonged exposure to the atrophy level in the range of 0 to 200 με results in decreased bone density. The hypertrophy level, which lies in the range of 2500 to 4000 με, stimulated remodeling activity, resulting in an increase in bone density. In addition, a fatigue failure level greater than 4000 με induces the generation of internal cracks that cannot be repaired by normal remodeling activity and might cause bone failure.[41] The von Mises stress was used to evaluate the stress distribution in the abutment, implant, and screw; von Mises interpretation was adequate for the analysis of a ductile material such as titanium.[42]

RESULTS

Figure 4 shows the maximum and minimum principal strain distributions representing the tensile and compressive strains in the surrounding bone induced by 4 different types of implants for vertical and oblique loading conditions. Strains mainly occurred in the buccal direction under vertical load and in the lingual direction under oblique load. The bone tissues in the fatigue failure level were observed in the alveolar ridge and in plateaus close to the implant apex. In the plateau tip, strains in the range of 2500 με or more (both hypertrophy and fatigue failure) were mostly observed, and the strain on the cortical and trabecular bone in the plateau tip was mostly greater than that in the groove. The results for vertical loading and oblique loading showed a similar distribution pattern around the peri-implant bone for all types of implant components; meanwhile, the maximum value and total volume of the overstrained bone tissue (hypertrophy and fatigue failure) under oblique loading were more than twice those under vertical loading (Fig. 5).

Under oblique loading, the sum of the bone volume in the hypertrophy and fatigue failure range induced by maximum and minimum principal strain was the largest for IB (8.79 mm^3) and the smallest for EB (4.26 mm^3). The total volume was similar for IT (6.31 mm^3) and ITW (6.38 mm^3). Under vertical loading conditions, the volume in the hypertrophy and fatigue failure levels was small for all types of implant components; the total volumes were 0.12 mm^3 (IT), 0.11 mm^3 (ITW), 0.05 mm^3 (IB), and 0.026 mm^3 (EB) (Table 2).

Figure 4 showed the maximum values (in magnitude) of the maximum and minimum principal strains observed in the cortical and trabecular bones. The maximum strain values were larger in the cortical bone than in the trabecular bone. In the cortical bone, the maximum (in magnitude) strain was induced by the compressive strain (minimum principal strain) for all implant types under both loading conditions, and oblique loading led to larger strains. IT and ITW exhibited the largest and

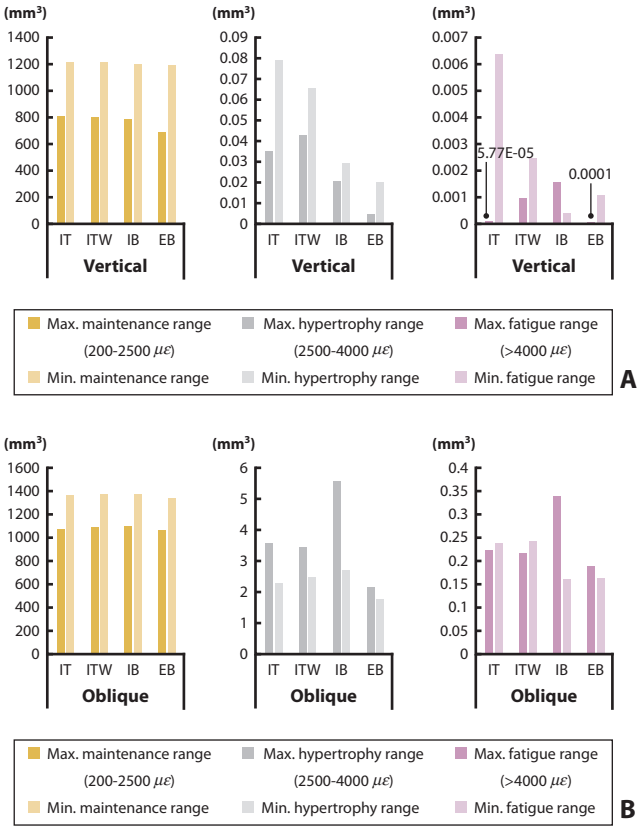

Figure 5. Bone volume according to maximum and minimum principal strain for 4 different types of short implant system under 2 loading conditions. A, Vertical loading condition. B, Oblique loading condition. EB, external bone level; IB, internal bone level; IT, internal tissue level; ITW, internal tissue level wide.

second-largest compressive strains under both vertical and oblique loadings, whereas EB and IB exhibited the smallest strains for oblique and vertical loading. Under oblique loading, the maximum strains (in magnitude) were −7678.1 με (IT), −6440.8 με (ITW), −5442.6 με (IB), and −5242.2 με (EB). Oblique loading provided larger maximum strains even in the trabecular bone; however, in trabecular bone, the maximum strain was induced mostly by the tensile strain for both the loading conditions. Under oblique loading, IB provided the largest maximum strain values (5856.8 με), whereas ITW provides the smallest (5619.7 με).

For all situations, the von Mises stress distribution of implant components presented a similar distribution pattern for each loading condition. Stress was concentrated in the buccal direction under vertical loading and in the lingual direction under oblique loading (Fig. 6).

For IT and ITW implant systems, the stress was concentrated in the region where the internal octagon abutment contacted the implant interior and in the region where the implant neck touched the cortical bone (Fig. 7). As IB possessed an internal-type abutment and bone level–type implant, stress was concentrated in the

Table 2. Bone volume according to maximum and minimum principal strain (value rounded)

Microstrain Range (με)		Vertical Load Condition (mm^3)				Oblique Load Condition (mm^3)			
		IT	ITW	IB	EB	IT	ITW	IB	EB
200 to 2500	Maximum	810	805	791	696	1080	1093	1097	1065
	Minimum	1218	1213	1199	1194	1360	1367	1373	1336
2500 to 4000	Maximum	0.04	0.04	0.02	0.05	3.57	3.44	5.58	2.15
	Minimum	0.08	0.07	0.03	0.02	2.27	2.47	2.70	1.75
>4000	Maximum	0.00	0.00	0.00	0.00	0.23	0.22	0.34	0.19
	Minimum	0.01	0.00	0.00	0.00	0.24	0.24	0.16	0.16

EB, external bone level; IB, internal bone level; IT, internal tissue level; ITW, internal tissue level wide.

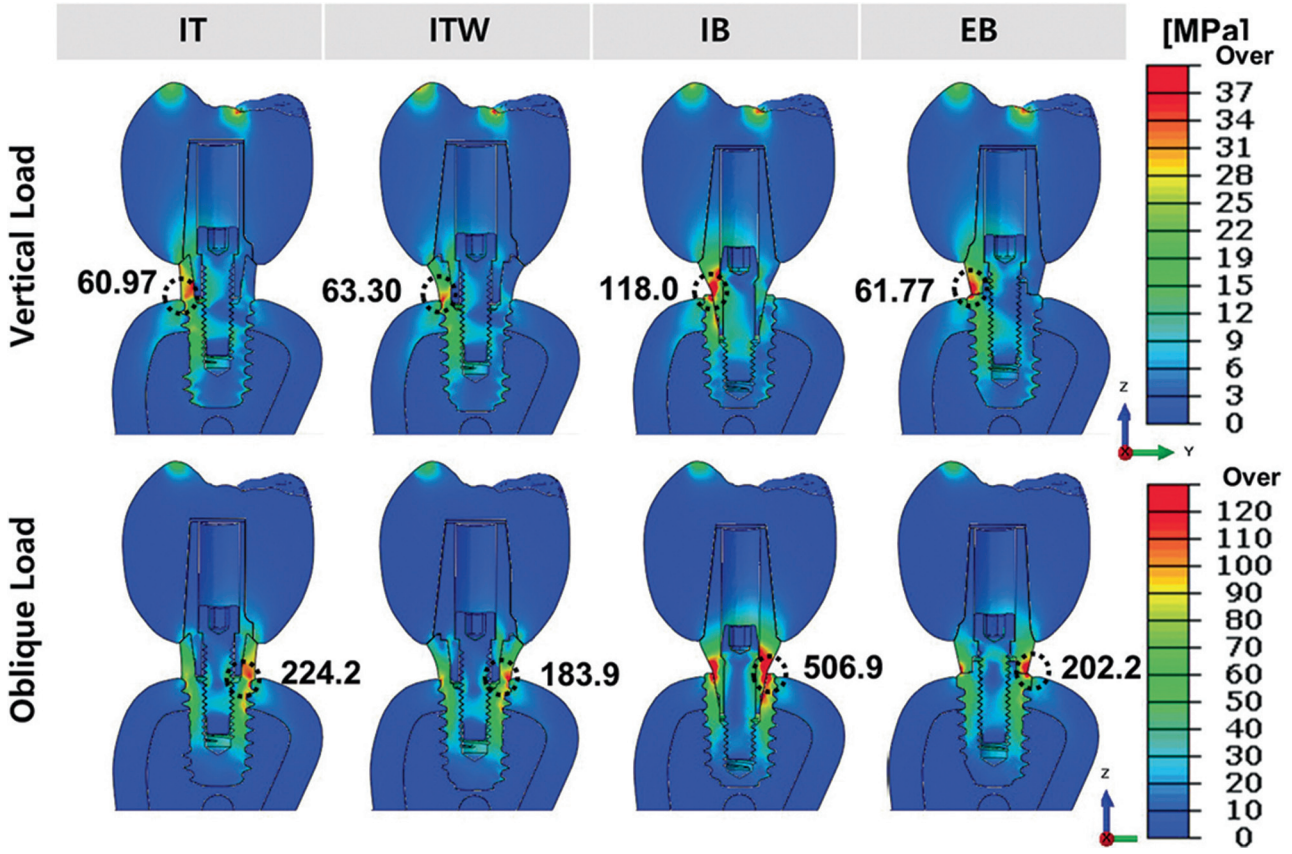

Figure 6. von Mises stress distribution of implant components and bone fragments showing location where stress concentration occurs under 2 loading conditions. EB, external bone level; IB, internal bone level; IT, internal tissue level; ITW, internal tissue level wide.

abutment at the conical seal, which is in contact with the screw and the implant-abutment surface. However, for the EB implant system, stress was concentrated in the abutment at the contact area between the top surface of the implant and external abutment.

Overall, oblique loading induced much higher stresses in the abutment, implant, and screw than vertical loading for all situations. The highest maximum stress of the abutment under oblique loading was observed in IB (506.9 MPa) and the lowest maximum stress in ITW (129.85 MPa). For the same loading condition, in the implant, the highest maximum stress was observed in IB (310.10 MPa) and the lowest in EB (175.72 MPa). For the screw, EB induced the highest maximum stress (160.2 MPa), whereas ITW had the lowest maximum stress (107.2 MPa) (Table 3).

Based on the static FE results of the titanium component for a tensile strength of 550 MPa, the computational fatigue analysis was performed to predict the risk of fracture caused by the fatigue accumulation of repetitive mastication in the vertical and oblique directions. In all situations, fracture was only predicted in the IB abutment model when oblique loading and vertical loading were performed alternately, and the number of life cycles of the IB abutment was 588 301. No damage was predicted for the other components within 10^7 loading cycles. For the abutment of IB, the crack was predicted in the lingual direction, which was the same

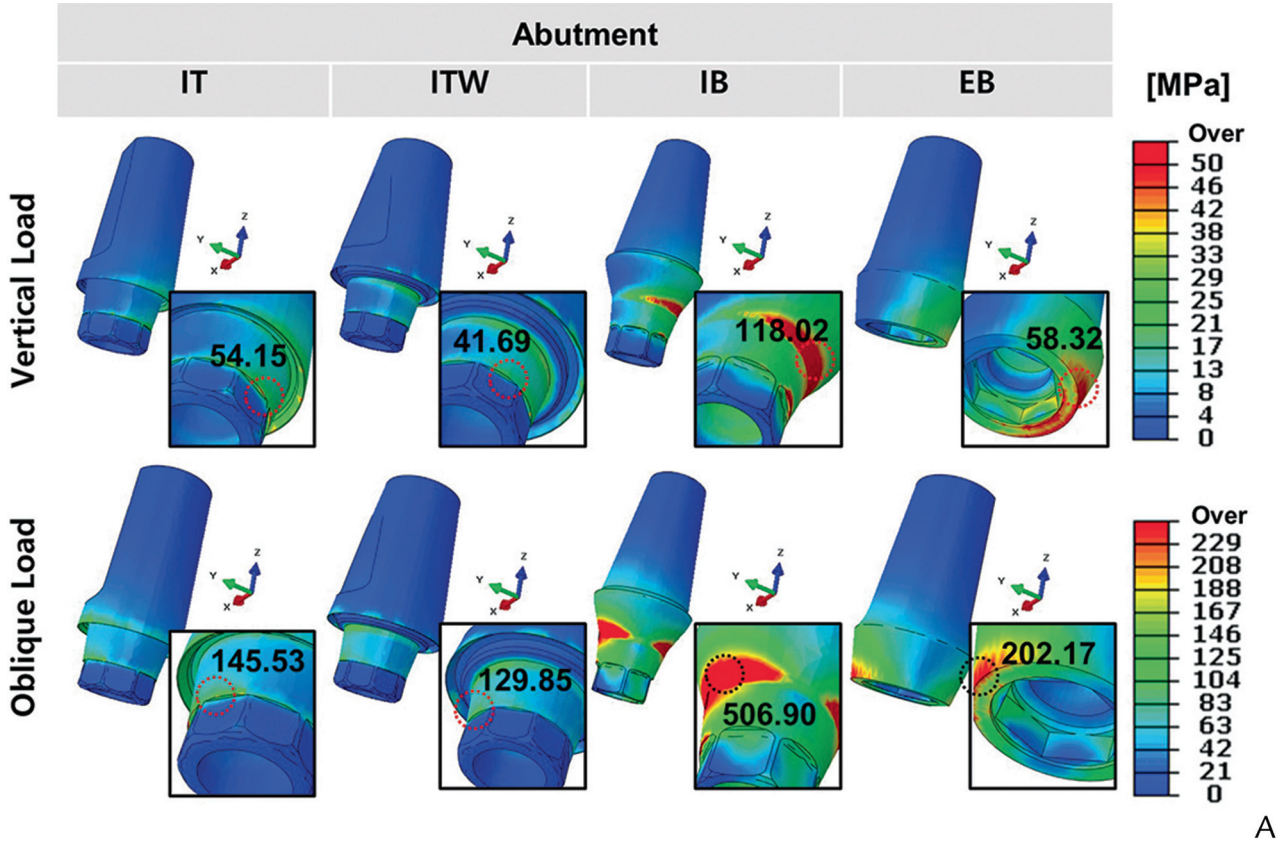

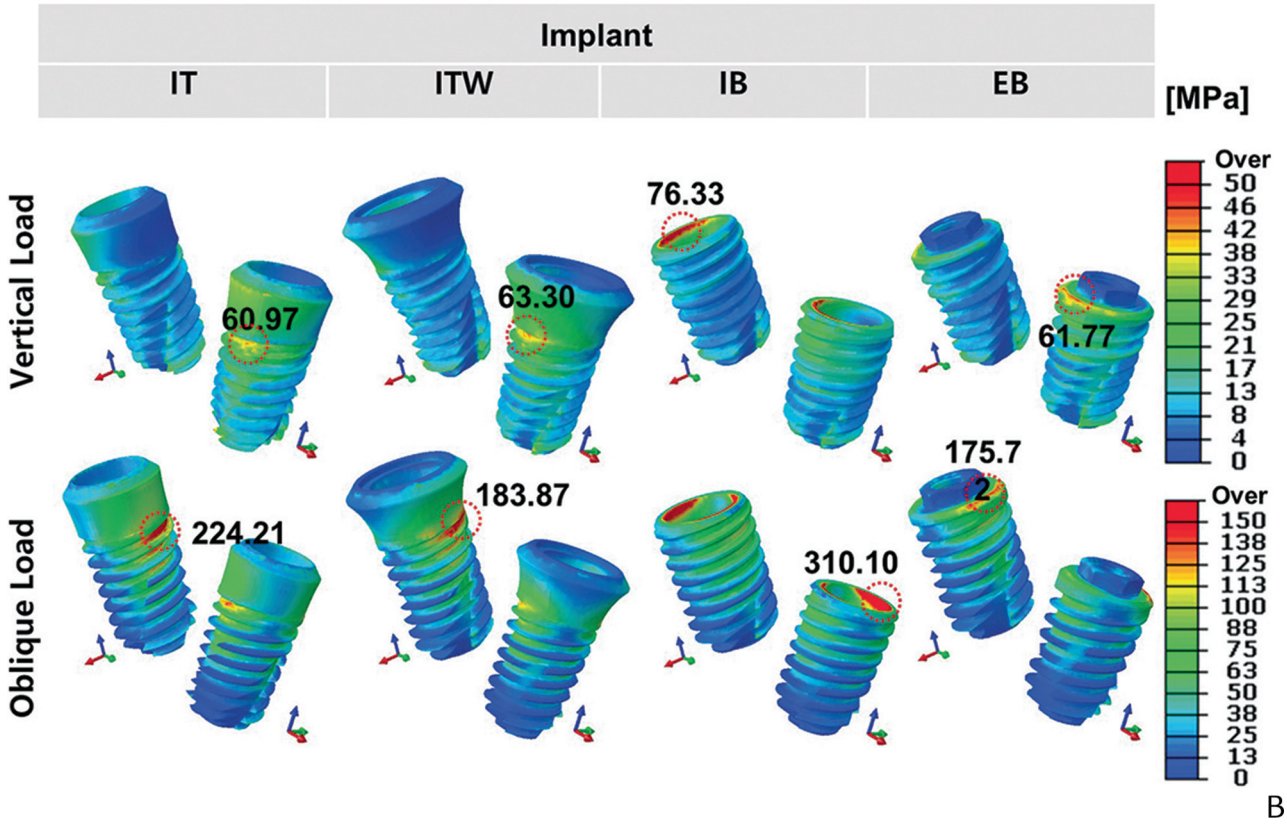

Figure 7. von Mises stress distribution and maximum value for abutment and implant showing location where stress concentration occurs under 2 loading conditions. (A) Stress distributions in the abutments, (B) stress distributions in the implants. EB, external bone level; IB, internal bone level; IT, internal tissue level; ITW, internal tissue level wide.

Table 3. Maximum von Mises stress in abutment, implant, and screw

Load Condition	Vertical Load Condition (MPa)				Oblique Load Condition (MPa)			
Implant System	**IT**	**ITW**	**IB**	**EB**	**IT**	**ITW**	**IB**	**EB**
Abutment	54	42	118	58	146	130	507	202
Implant	61	63	76	62	224	184	311	176
Screw	32	27	44	54	128	107	145	160

EB, external bone level; IB, internal bone level; IT, internal tissue level; ITW, internal tissue level wide.

direction along which the stress was concentrated under oblique loading (Fig. 8).

DISCUSSION

The results of the present study revealed that the stress distributions in the implant components and the strain distribution in the bone are noticeably affected by the connection type. Therefore, the null hypothesis that all the connection types would produce similar stress and strain distributions was rejected.

Although the yield strength of the implant and abutment has been reported to be acceptably high, mechanical failure of the implant components can still occur under different conditions. Studies that have determined the level of strain surrounding the bone that would lead to the failure of osseointegration of the implant are sparce.[29,43] Most bones are more durable under compressive strain than tensile strain[44] and do not fracture until around 25 000 με, according to the Frost mechanostat theory.[43,45]

In this study, bone strain values were 2 to 3 times higher under oblique loading than those under vertical loading. IT exhibited the maximum strain (7678.1 με) in the cortical bone under oblique loading (Fig. 4), which is in excess of the lower limit of fatigue failure. However, the bone volume in the fatigue failure range was only 0.34 mm^3, which occupies an extremely small portion of the whole (Table 2). Whenever masticatory force is applied intraorally, the location of failure over 4000 με would be different. Even if there is a microfracture in a very small area around the implant, it might be able to heal because of the short duration of application of the masticatory force, which is around 9 minutes in a day.[46] A small difference was found in the strain values under vertical loading according to different connections; however, with regard to the cortical bone under oblique loading, the strain in IT was around 1.8 times higher than that in IB, which was the greatest difference among all groups.

Although the strain values of bone were physiologically acceptable under all conditions, the lever effect from lateral force was the major factor contributing to the increase in the strain on the bone and should be considered to be a severe high-lever effect. It could be close to the fracture risk range with an excessive crown height and increased lateral force because of bruxism.

The force and area of the contact influence stress. A lower force and larger area of contact reduce the stress, which minimizes mechanical failure of the implant prosthesis. When an equal masticatory force is applied to a prosthesis with different connections, a different force is generated according to the length of the effort arm and resistance arm. An increased crown height results in an increase in the length of the effort arm, which would escalate the force.[28] The crown of a tissue-level implant is structurally shorter than that of a bone-level implant and is as much as the length of the transmucosal part. Therefore, a tissue-level implant has a mechanical advantage over a bone-level implant. The area of contact is another factor of stress. If an abutment is thick and wide, the stress is decreased under the same loading condition.

In this study, IB and EB had a similarly long effort arm. However, the stress of the abutment of IB was 2.5 times higher than that of EB, which could have been caused by the difference in the structural thickness of the abutment and the different lengths of the resistance arm. The stress of the abutment in IB was 3.5 times higher than that of IT. In bone-level connections, masticatory force is transmitted through the abutment to the implant; all the stress of the implant is carried through the engaging surface between the implant and abutment only. In a tissue-level connection, some part of the force is directly dispersed to the platform of implant as well as the abutment due to the direct contact between the crown and implant, which could decrease the stress of the abutment and screw.

Balik et al[8] observed the maximum stress on the implant in several different connections. Under 111 N of 30-degree oblique loading, a tissue-level implant with a similar design to that of the IT showed a maximum stress of 120 MPa. It would provide about 218 MPa under the 200-N force as used in this study; the value is close to the stress value of the implant (224 MPa) of the IT calculated in this study.

In the implants, stress was concentrated on the tightly engaged contact area between the implant and abutment in the bone-level implant, whereas it was concentrated on the first thread area below the transmucosal part (Figs. 6 and 7). The thin part of the implant experiences peak stress, as shown in the sectional view (Fig. 6).

Masticatory movement varies in different individuals, making it difficult to reproduce with only a single vertical movement or a single oblique movement. In this study, the combination of 1 vertical and 1 oblique loading was defined as a set of cyclic loading to simulate real movement rather than simple movement in 1 direction. Therefore, 588 301 load cycles for fracture of the abutment of IB could be assumed to be around 1 200 000 under each loading condition, which corresponds to 5 years of masticatory movement.[47]

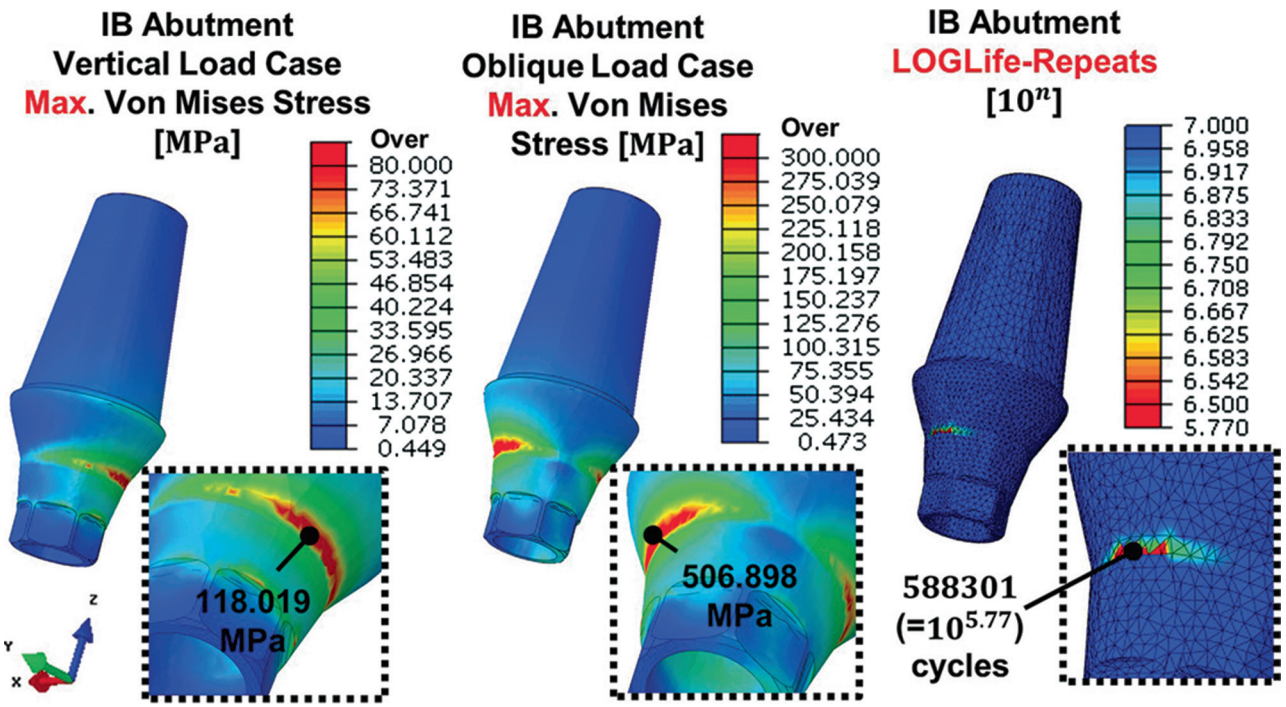

Figure 8. Left: stress distribution of abutment of IB under vertical loading condition; Middle: stress distribution of abutment of IB under oblique loading condition; Right: location where fracture occurs as result of fatigue of IB abutment under cyclic loading condition consisting of one 200-N vertical and one 200-N oblique loading. IB, internal bone level.

The abutment in this study was modeled from grade 4 titanium. Of the various grades of titanium available for abutments, grades 4 and 5 are widely available in the market.[48] As demonstrated by many studies, titanium grade 5 abutments exhibit higher strength than grade 4 abutments because the yield strength is 785 MPa for the grade 5 and 483 MPa for the grade 4.[48-50] Therefore, the titanium grade of the abutment needs to be considered carefully in IB implants, especially those with narrow connections which exhibit high stress as compared with other types of connection.

The stress on the implant, abutment, and screw was influenced by the difference in the connection and loading conditions. The mean stress in all implant components for all groups under oblique loading was 3.5 times higher than that under vertical loading; meanwhile, the stress of IB was 2.16 times higher than that of ITW, which is the highest difference among all groups (Fig. 9). Different connections lead to different lever effects, which are defined by the ratio of the length of the effort arm to that of the resistance arm. The stress on the implant will decrease if the inclination of the cusp is decreased, which would prevent the high lateral force from loading. The highest stress of the IB implant (310 MPa) in this study was for a crown height of 13 mm and 30-degree oblique loading under 200 N, which is around 56% to 67% of the yield strength of Ti-grade 4 implant.[51] However, the highest stress could be larger than the yield strength in more challenging clinical situations.

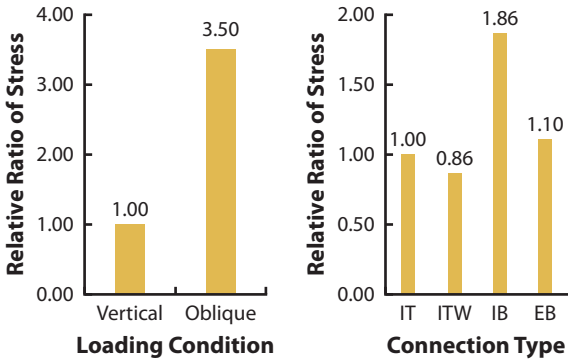

Figure 9. Relative ratio of stress with loading and relative ratio of stress with different connections. EB, external bone level; IB, internal bone level; IT, internal tissue level; ITW, internal tissue level wide.

All the components in this study were assumed to be isotropic, homogenous, and linearly elastic, and perfect osseointegration was also assumed. The computational model used in this study may not fully represent the real situation because there are additional factors that are difficult to predict, such as flaws, nonlinear deformation, or intrinsic preload. Also, for the resorbed mandible with largely different dimensions or abnormal bone conditions, the result may not be valid. Therefore, the results need to be interpreted with caution. Although we performed the analysis only with the vertical and oblique occulusal loadings in this study, further studies with near

horizontal loadings induced by mandibular advancement devices would also be of value.

CONCLUSIONS

Based on the findings of this FEA study, the following conclusions were drawn:

1. The abutment of IB showed the highest stress of the implant component, whereas IT showed the highest strain of bone.
2. Bone strain values for all groups appeared within physiologic capacity.
3. Different mechanical situations should be considered when using IB connections in short implants on the posterior area.

REFERENCES

1. Nisand D, Picard N, Rocchietta I. Short implants compared to implants in vertically augmented bone: a systematic review. Clin Oral Implants Res 2015;26:170-9.
2. Thoma DS, Zeltner M, Husler J, Hammerle CH, Jung RE. EAO Supplement Working Group 4 - EAO CC 2015 Short implants versus sinus lifting with longer implants to restore the posterior maxilla: a systematic review. Clin Oral Implants Res 2015;26:154-69.
3. Hanaoka M, Gehrke SA, Mardegan F, Gennari CR, Taschieri S, Rabbro MD, et al. Influence of implant/abutment connection on stress distribution to implant-surrounding bone: a finite element analysis. J Prosthodont 2014;23:565-71.
4. Faria Almeida DA, Pellizzer EP, Verri FR, Santiago JF Jr, Carvalho PS. Influence of tapered and external hexagon connections on bone stresses around tilted dental implants: three-dimensional finite element method with statistical analysis. J Periodontol 2014;85:261-9.
5. Borie E, Orsi IA, Noritomi PY, Kemmoku DT. Three-dimensional finite element analysis of the biomechanical behaviors of implants with different connections, lengths, and diameters placed in the maxillary anterior region. J Oral Maxillofac Implants 2016;31:101-10.
6. Santiago JF Jr, Verri FR, Almeida DA, Souza Batista VE, Lemos CA, Pellizzer EP. Finite element analysis on influence of implant surface treatments, connection and bone types. Mater Sci Eng C Mater Biol 2016;63:292-300.
7. Covani U, Ricci M, Tonelli P, Barone A. An evaluation of new designs in implant-abutment connections: a finite element method assessment. Implant Dent 2013;22:263-7.
8. Balik A, Karatas MO, Keskin H. Effects of different abutment connection designs on the stress distribution around five different implants: a 3-dimensional finite element analysis. J Oral Implantol 2012;38:491-6.
9. Anami LC, da Costa Lima JM, Takahashi FE, Neisser MP, Noritomi PY, Bottino MA. Stress distribution around osseointegrated implants with different internal-cone connections: photoelastic and finite element analysis. J Oral Implantol 2015;41:155-62.
10. Pessoa RS, Muraru L, Junior EM, Vaz LG, Sloten JV, Duyck J, et al. Influence of implant connection type on the biomechanical environment of immediately placed implants - CT-based nonlinear, three-dimensional finite element analysis. Clin Implant Dent Relat Res 2010;12:219-34.
11. Sugiura T, Yamamoto K, Horita S, Murakami K, Kirita T. Micromotion analysis of different implant configuration, bone density, and cortical bone thickness in immediately loaded mandibular full-arch implant restorations: a nonlinear finite element study. Clin Implant Dent Relat Res 2017;20:43-9.
12. Pessoa RS, Coelho PG, Muraru L, Marcantonio E Jr, Geraldo VL, Vander SJ, et al. Influence of implant design on the biomechanical environment of immediately placed implants: computed tomography-based nonlinear three-dimensional finite element analysis. Int J Oral Maxillofac Implants 2011;26:1279-87.
13. Tsouknidas A, Lympoudi E, Michalakis K, Giannopoulos D, Michailidis N, Pissiotis A, et al. Influence of alveolar bone loss and different alloys on the biomechanical behavior of internal-and external-connection implants: a three-dimensional finite element analysis. Int J Oral Maxillofac Implants 2015;30:30-42.
14. Jimbo R, Halldin A, Janda M, Wennerberg A, Vandeweghe S. Vertical fracture and marginal bone loss of internal-connection implants: a finite element analysis. Int J Oral Maxillofac Implants 2013;28:171-6.
15. Sannino G, Barlattani A. Mechanical evaluation of an implant-abutment self-locking taper connection: finite element analysis and experimental tests. Int J Oral Maxillofac Implants 2013;28:17-26.
16. Choi KS, Park SH, Lee JH, Jeon YC, Yun MJ, Jeong CM. Stress distribution on scalloped implants with different microthread and connection configurations using three-dimensional finite element analysis. Int J Oral Maxillofac Implants 2012;27:29-38.
17. Ramos VF, Santiago JF Jr, de Faria Almeida DA, de Oliceira GBB, de Souza Batista VE, Honorio HM, et al. Biomechanical influence of crown-to-implant ratio on stress distribution over internal hexagon short implant: 3-D finite element analysis with statistical test. J Biomech 2015;48:138-45.
18. Isidor F. Influence of forces on peri-implant bone. Clin Oral Implants Res 2006;17:8-18.
19. Rangert B, Krogh PH, Langer B, Van Roekel N. Bending overload and implant fracture: a retrospective clinical analysis. Int J Oral Maxillofac Implants 1995;10:326-34.
20. Song HY, Huh YH, Park CJ, Cho LR. A two-short-implant-supported molar restoration in atrophic posterior maxilla: a finite element analysis. J Adv Prosthodont 2016;8:304-12.
21. Lee KJ, Kim YG, Park JW, Lee JM, Suh JY. Influence of crown-to-implant ratio on periimplant marginal bone loss in the posterior region: a five-year retrospective study. J Periodontal Implant Sci 2012;42:231-6.
22. Garaicoa-Pazmino C, Suarez-Lopez del Amo F, Monje A, Catena A, Ortega-Oller I, Galindo-Moreno P, et al. Influence of crown/implant ratio on marginal bone loss: a systematic review. J Periodontol 2014;85:1214-21.
23. Glantz PO, Nilner K. Biomechanical aspects of prosthetic implant-borne reconstructions. Periodontol 2000 1998;17:119-24.
24. Malchiodi L, Cucchi A, Ghensi P, Consonni D, Nocini PF. Influence of crown-implant ratio on implant success rates and crestal bone levels: a 36-month follow-up prospective study. Clin Oral Implants Res 2014;25:240-51.
25. Tawil G, Aboujaoude N, Younan R. Influence of prosthetic parameters on the survival and complication rates of short implants. Intl J Oral Maxillofac Implants 2006;21:275-82.
26. Schulte J, Flores AM, Weed M. Crown-to-implant ratios of single tooth implant-supported restorations. J Prosthet Dent 2007;98:1-5.
27. Blanes RJ, Bernard JP, Blanes ZM, Belser UC. A 10-year prospective study of ITI dental implants placed in the posterior region. II: influence of the crown-to-implant ratio and different prosthetic treatment modalities on crestal bone loss. Clin Oral Implants Res 2007;18:707-14.
28. Bulaqi HA, Mousavi Mashhadi M, Safari H, Samandari MM, Geramipanah F. Effect of increased crown height on stress distribution in short dental implant components and their surrounding bone: a finite element analysis. J Prosthet Dent 2015;113:548-57.
29. Anitua E, Alkhraist MH, Pinas L, Begona L, Orive G. Implant survival and crestal bone loss around extra-short implants supporting a fixed denture: the effect of crown height space, crown-to-implant ratio, and offset placement of the prosthesis. Int J Oral Maxillofac Implants 2014;29:682-9.
30. Papakoststas GI, Mcgrath P, Stewart J, Charles D, Chen Y, Mischoulon D, et al. Psychic and somatic anxiety symptoms as predictors of response to fluoxetine in major depressive disorder. Psychiatry Res 2008;161:116-20.
31. Vaillancourt H, Pilliar RM, Mccammond D. Finite-element analysis of crestal bone loss around porous-coated dental implants. J Appl Biomater 1995;6:267-82.
32. Bulaqi HA, Mashhadi MM, Safari H, Samandari MM, Geramipanah F. Effect of increased crown height on stress distribution in short dental implant components and their surrounding bone: a finite element analysis. J Prosthet Dent 2015;113:548-57.
33. Niinomi M. Mechanical properties of biomedical titanium alloys. Mater Sci Eng 1998;243:231-6.
34. Sertgoz A. Finite element analysis study of the effect of superstructure material on stress distribution in an implant-supported fixed prosthesis. Int J Prosthodont 1997;10:19-27.
35. Sevimay M, Turhan F, Kilicarslan MA, Eskitascioglu G. Three-dimensional finite element analysis of the effect of different bone quality on stress distribution in an implant-supported crown. J Prosthet Dent 2005;93:227-34.
36. Tolidis K, Papadogiannis D, Papadogiannis Y, Gerasimou P. Dynamic and static mechanical analysis of resin luting cements. J Mech Behav Biomed Mater 2012;6:1-8.
37. Guda T, Ross TA, Lang LA, Millwater HR. Probabilistic analysis of preload in the abutment screw of a dental implant complex. J Prosthet Dent 2008;100:183-93.
38. Mornegurg TR, Proschel P. In vivo forces on implants influenced by occlusal scheme and food consistency. Int J Prosthodont 2003;16:481-6.
39. Rodriguez AM, Aquilino SA, Lund PS. Cantilever and implant biomechanics: a review of the literature, part I. J Prosthodont 1994;3:41-6.
40. Wierszycki M, Kąkol W, Lodygowski T. The screw loosening and fatigue analyses of three dimensional dental implant model. ABAQUS Users' Conference 2006;527-541.
41. Roberts WE, Huja S, Roberts JA. Bone modeling: biomechanics, molecular mechanisms, and clinical perspectives. Semin Orthod 2004;10:123-61.
42. Barao VA, Delben JA, Lima J, Cabral T, Assuncao WG. Comparison of different designs of implant-retained overdentures and fixed full-arch

implant-supported prosthesis on stress distribution in edentulous mandible–a computed tomography-based three-dimensional finite element analysis. J Biomech 2013;46:1312-20.
43. Naert I, Duyck J, Vandamme K. Occlusal overload and bone/implant loss. Clin Oral Implants Res 2012;23:95-107.
44. Keaveny TM, Wachtel EF, Ford CM, Hayes WC. Differences between the tensile and compressive strengths of bovine tibial trabecular bone depend on modulus. J Biomech 1994;27:1137-46.
45. Tyrovola JB. The "Mechanostat Theory" of Frost and the OPG/RANKL/RANK System. J Cell Biochem 2015;116:2724-9.
46. Graf H. Bruxism. Dent Clin North Am 1969;13:659-65.
47. DeLong R, Douglas WH. Development of an artificial oral environment for the testing of dental restoratives: bi-axial force and movement control. J Dent Res 1983;62:32-6.
48. Park SJ, Lee SW, Leesungbok R, Ahn SJ. Influence of the connection design and titanium grades of the implant complex on resistance under static loading. J Adv Prosthodont 2016;8:388-95.
49. Gigandet M, Bigolin G, Faoro F, Burgin W, Bragger U. Implants with original and non-original abutment connections. Clin Implant Dent Relat Res 2014;16:303-11.
50. Jo JY, Yang DS, Huh JB, Heo JC, Yun MJ, Jeong CM. Influence of abutment materials on the implant-abutment joint stability in internal conical connection type implant systems. J Adv Prosthodont 2014;6:491-7.
51. Welsch F, Boyer F, Collings EW. Materials properties handbook: titanium alloys. 1st ed. Materials Park: ASM International; 1994. p. 483-633.

Corresponding author:
Dr Gunwoo Noh
School of Mechanical Engineering
Kyungpook National University
1370 Sankyuk Dong, Buk-gu
Daegu 41566
REPUBLIC OF KOREA
Email: gunwoo@knu.ac.kr

https://doi.org/10.1016/j.prosdent.2018.07.013